

Loss-of-Function Homozygous Variant in *LPL* Causes Type I Hyperlipoproteinemia and Renal Lipidosis



Hongyan Wu¹, Huan Xu², Song Lei², Zhi Yang¹, Shan Yang¹, Jingxue Du¹, Yi Zhou¹, Yunqiang Liu³, Yuan Yang³ and Zhangxue Hu¹

¹Department of Nephrology, West China Hospital, Sichuan University, Chengdu, China; ²Department of Pathology, West China Hospital, Sichuan University, Chengdu, China; and ³Department of Medical Genetics, West China Hospital, Sichuan University, Chengdu, China

Introduction: Lipoprotein lipase (LPL) is an important enzyme in lipid metabolism, individuals with *LPL* gene variants could present type I hyperlipoproteinemia, lipemia retinalis, hepatosplenomegaly, and pancreatitis. To date, there are no reports of renal lipidosis induced by type I hyperlipoproteinemia due to *LPL* mutation.

Methods: Renal biopsy was conducted to confirm the etiological factor of nephrotic syndrome in a 44-year-old Chinese man. Lipoprotein electrophoresis, *apoE* genotype detection, and whole-exome sequencing were performed to confirm the dyslipidemia type and genetic factor. Analysis of the 3-dimensional protein structure and *in vitro* functional study were conducted to verify variant pathogenicity.

Results: Renal biopsy revealed numerous CD68 positive foam cells infiltrated in the glomeruli; immunoglobulin and complement staining were negative; and electron microscopy revealed numerous lipid droplets and cholesterol clefts in the cytoplasm of foam cells. Lipoprotein electrophoresis revealed that the patient fulfilled the diagnostic criteria of type I hyperlipoproteinemia. The *apoE* genotype of the patient was the $\epsilon 3/\epsilon 3$ genotype. Whole-exome sequencing revealed an *LPL* (c.292G > A, p.A98T) homozygous variant with α -helix instability and reduced post-heparin LPL activity but normal lipid uptake capability compared to the wild-type variant.

Conclusion: *LPL* (c.292G > A, p.A98T) is a pathogenic variant that causes renal lipidosis associated with type I hyperlipoproteinemia. This study provides adequate evidence of the causal relationship between dyslipidemia and renal lesions. However, further research is needed to better understand the pathogenetic mechanism of *LPL* variant-related renal lesions.

Kidney Int Rep (2023) 8, 2428–2438; <https://doi.org/10.1016/j.ekir.2023.08.027>

KEYWORDS: cholesterol clefts; foam cell; homozygous variant; lipoprotein lipase; renal lipidosis; type I hyperlipoproteinemia

© 2023 International Society of Nephrology. Published by Elsevier Inc. This is an open access article under the CC BY-NC-ND license (<http://creativecommons.org/licenses/by-nc-nd/4.0/>).

Lipoprotein lipase is a secretory protein that hydrolyzes triglycerides (TGs) in TG-rich chylomicrons and very-low-density lipoproteins. Various studies indicate that impaired LPL activity due to an *LPL* gene variant results in massive accumulation of chylomicrons and fasting hypertriglyceridemia.^{1–3} To date, more than 220 *LPL* variants related to hypertriglyceridemia have been identified, and most of these variants are distributed in exons 4, 5, and 6.^{4,5} It is indicated that 60% of LPL deficiency-causing

mutations are missense mutations; however, nonsense, deletion, insertion, splicing, and other types of mutations have also been reported.^{3,4,6–17}

Homozygous deficiency of LPL is rare, with a frequency of 1 per million in general populations. Homozygous and compound heterozygous mutations in the *LPL* gene may cause severe hypertriglyceridemia due to complete or partial loss of LPL activity.^{10,18,19} *APOC2*, *APOA5*, *LMFI*, *GPIHBP1*, *ANGPTL3*, and *ANGPTL4* are also involved in the regulation of LPL activity, except for *LPL* gene mutation.^{1,2,9,10,20} Individuals with LPL activity deficiency typically present with type I hyperlipoproteinemia, recurrent abdominal pain, eruptive xanthomas, lipemia retinalis, hepatosplenomegaly, and pancreatitis.^{6,11,12} However, there has been no report of renal lesion induced by the *LPL* homozygous variant. In this study, we report an *LPL* (c.292G > A, p.A98T)

Correspondence: Zhangxue Hu, Department of Nephrology, West China Hospital, Sichuan University, Guoxue Alley, 37#, Wuhou District, Chengdu, Sichuan Province, 610041, China. E-mail: hzxawy@scu.edu.cn

Received 11 April 2023; revised 5 August 2023; accepted 22 August 2023; published online 25 August 2023

homozygous variant with obvious renal lipodosis. To further investigate the pathogenesis of the renal lesion, we conducted an *in vitro* functional study.

METHODS

Lipoprotein Electrophoresis

Plasma lipoproteins were separated using a commercial SPIFE lipoprotein kit (cat.3341, Helena Laboratories, Beaumont, TX), which is different in formulation from the traditional lipoprotein kit. On the SPIFE lipoprotein gel, chylomicrons stay at the loading point, but beta-lipoproteins migrate slightly cathodal to the loading point.²¹ The Quick Scan 2000 software (cat.1660, Helena Laboratories) was used for lipoprotein electrophoresis band analysis.

Whole-Exome Sequencing

The genomic DNA of the patient was extracted and fragmented by nebulization, and the fragmented DNA was end-repaired and A-tailed using standard protocols. Illumina adapters were ligated to the A-tailed fragments, and the products were size-selected for a 350-base to 400-base pair product. Whole-exome enrichment was performed using the GenCap custom enrichment kit (MyGenostics Inc, Beijing, China) according to the manufacturer's protocol. The biotinylated capture probes (80–120 mer) were designed to tile all the exons with nonrepeated regions and sequenced on an Illumina NextSeq 500 sequencer (Illumina, San Diego, CA) for paired-end reads of 150 bp.

Pathogenicity and Protein Structure Analysis of Mutant LPL

Sequence alignment of the human LPL protein (NP_000228.1) was performed using DNASTar-MegAlign software (<http://www.dnastar.com/t-megalign.aspx>). Pathogenicity was assessed using Polyphen-2 software (<http://genetics.bwh.harvard.edu/pph2/>) and PROVEAN (<http://provean.jcvi.org/index.php>). Protein structures were generated using Swiss-PdbViewer 4.0 software (<http://www.expasy.org/spdbv/>) by the method of homology modeling.

Plasmids Construction and Transfection

Human wild type *LPL* cDNA (NM_000237) and c.292G>A *LPL* cDNA were synthesized and cloned into the pEZ-M45 vector with a HA tag at the C-terminus by GeneCopoeia (Rockville, MD). The 293T cells and RAW264.7 macrophages were kindly provided by Stem Cell Bank, Chinese Academy of Sciences and cultured in DMEM high-glucose medium supplemented with 10% fetal bovine serum, penicillin (100 U/ml), and streptomycin (100 µg/ml) at 37 °C in 5% CO₂. Expression plasmids containing the human wild type *LPL* and mutant *LPL*

were transfected into the RAW264.7 and 293T cells by jetOPTIMUS DNA transfection reagent (117-07, Polyplus Transfection, Illkirch, France), pEZ-M45 was used as a negative control plasmid.

Measurement of LPL Activity and Mass

To analyze the activity and mass of LPL, heparin was added to trigger the release of cell surface-bound LPL into the cell medium. After 36 hours of transfection, the cell medium of 293T cells was changed to a heparin-optiMEM mixture (for a final heparin concentration of 20 units/ml per well) and incubated for 30 minutes. The post-heparin cell culture medium and cell lysate were then harvested. LPL mass and activity were determined using human LPL ELISA kit (MM-0468H1, MEIMIAN, China) and LPL activity assay kit (BC2445, Solarbio, China), respectively.

Lipid Uptake and Oil Red O Staining of RAW264.7 Cells

After 24 hours of transfection, 30 µg/ml dil-oxLDL (YB-0010, Yiyuan Biotech, China) was added to the serum-free medium and incubated for 5 hours to evaluate the lipid uptake capability of various transfected RAW264.7 cells by fluorescence microscope. The fluorescence intensity of dil-oxLDL-positive cells was calculated using the Image J software (National Institute of Health, Bethesda, MD).

In addition, after 24 hours of transfection, the RAW264.7 cells were incubated with 25 µg/mL ox-LDL (YB-002, Yiyuan Biotech, China) in a serum-free medium for an additional 12 hours. Thereafter, the cells were stained with the Oil red O reagent (G1262, Solarbio, China) to identify foam cell formation.

Western Blotting Analysis

Western blotting analyses were performed as previously described using 20 µg lysates from RAW264.7 and 293T cells.²² Antibody used for western blotting include mouse anti-HA (A5969, Bimake, China), rabbit anti-GAPDH (380626, Zen Bio, China), antimouse HRP secondary (#7076, Cell Signaling Technology, Danvers, MA), antirabbit HRP secondary (#7074, Cell Signaling Technology, Danvers, MA); all antibodies were diluted in 5% bovine serum albumin or 5% nonfat milk in TBST. Target protein bands were captured using a chemiluminescence imager (iBright CL1000; Thermo Fisher Scientific, Waltham, MA).

Reverse Transcription-Quantitative Polymerase Chain Reaction (PCR)

Real-time PCR was performed as previously described.²² HiScript II Q RT SuperMix (R223-01, Vazyme, China) and TB Green Premix Ex Taq II kit (RR820A, TaKaRa Bio, China) were used to perform the quantitative PCR. The

Table 1. Primer sequences for qPCR

Gene	Sense (5' → 3')	Anti-sense (5' → 3')
LPL (human)	TCATTCCCGGAGTAGCAGAGT	GGCCACAAGTTTTGGCACC
GAPDH (mouse)	TGTTTCTCGTCCCGTAGA	ATCTCCACTTTGCCACTGC
GAPDH (human)	GGAGCGAGATCCCTCCAAAAT	GGCTGTTGTCATACTTCTCATGG

GAPDH, glyceraldehyde-3-phosphate dehydrogenase; LPL, lipoprotein lipase.

results were obtained using a CFX96 Real-Time PCR detection system (Bio-Rad, Hercules, CA) with the following program design: a denaturation step at 95 °C for 30 seconds, followed by 40 cycles of denaturation at 95 °C for 5 seconds, annealing at 57 °C for 30 seconds, and extension at 72 °C for 30 seconds. The sequences of primer pairs are shown in Table 1.

Statistical Analysis

Statistical analysis was performed using the GraphPad Prism 7 software (GraphPad Software Inc., San Diego, CA). Data are presented as mean ± SD, and 1-way analysis of variance was used to compare mean values between 3 groups. No significance (NS) indicates $P > 0.05$; * $P < 0.05$; ** $P < 0.01$; *** $P < 0.001$; and **** $P < 0.0001$.

RESULTS

Case Presentation

A 44-year-old Chinese man was admitted to our hospital in November 2014 for facial and lower extremity edema; recurrent episodes of pancreatitis and peritonitis were present in past medical history, and family history of hyperlipemia was denied. On admission, physical examination of the patient revealed that his blood pressure was 152/100 mmHg. His height was 165 cm, weight was 73 kg (body mass index = 26.8 kg/m²). Laboratory analysis revealed hemoglobin level of 10.4 g/dl, serum creatinine level of 1.38 mg/dl, urea nitrogen level of 25.4 mg/dl, serum albumin level of 1.54 g/dl, TG level of 1056.7 mg/dl, serum cholesterol level of 231 mg/dl, low-density lipoprotein cholesterol level of 38.3 mg/dl, high-density lipoprotein cholesterol level of 27.09 mg/dl, apoA1 level of 1.21 g/l, apoB100 level of 0.86 g/l, apoE level of 13.5 mg/dl, blood glucose level of 4.78mmol/l, and HbA1c was 4.5%. The fasting plasma of the patient had a markedly creamy layer; lipoprotein electrophoresis revealed the characteristic of type I hyperlipoproteinemia with obvious chylomicron band in loading point (Figure 1). Urinary protein level was 4.08 g/24h, urinary sediment level was 49 red blood cells per high-power field. Serum rheumatoid factor level was 43.2 IU/ml; however, serum antinuclear antibody test, antidouble-stranded DNA test, antineutrophil cytoplasmic antibody test, and antiglomerular basement membrane test were all negative. Serum C3 level was

81.8 mg/dl, and serum C4 level was 66.6 mg/dl. Serum immunofixation electrophoresis did not reveal monoclonal immunoglobulin. Serum cryoglobulin test was negative. Ultrasonic testing revealed that splenomegaly and both kidneys were enlarged.

Renal biopsy was performed. Of the 21 glomeruli sampled for light microscopy, none were globally sclerotic or segmentally sclerotic. No crescents were found. Extensive CD68+ foam cells infiltration with moderate-to-severe increase in mesangial cell number and matrix (with segmental mesangial interposition and duplication of glomerular basement membranes) in glomeruli was observed. Sudan III and Oil red O staining were positive. Tubular atrophy and interstitial fibrosis were observed in about 5% of the sampled cortices. There were no obvious vascular lesions. Immunoglobulin and complement stains were negative. Electron microscopy revealed numerous lipid droplets and cholesterol clefts in the cytoplasm of foam cells (Figure 2).

Whole-Exome Sequencing and Protein Structure Prediction

The apoE genotype of the patient was ε3/ε3 genotype. Whole-exome sequencing revealed a rare homozygous mutation of the *LPL* gene (c.292G > A, p.A98T) in the patient, and this homozygous variant was rarely found in the Exome Variant Server, 1000 Genomes Project, and Exome Aggregation Consortium databases (Figure 3). In addition to *LPL*, *APOC2*, *APOA5*, *LMF1*, and *GPIHBP1* did not have pathogenic mutations. Amino acid sequence alignment of *LPL* in a variety of species showed that the amino acid residue Ala98 is highly conserved in *LPL* orthologs.

Analysis using PROVEAN and Polyphen-2 revealed that this missense variant may be damaging (score: -3.325 and score: 1.00, respectively). The 3-dimensional structure showed that the amino acid residue 98 was located in a region annotated in UniProt to form an α-helix and close to the first loop (residue 91–95) of *LPL*. As shown in Figure 4, substitution of threonine for alanine at this site could increase the number of H-bonds between LYS94 and THR98 or between LEU95 and THR98, thereby affecting the stability of the α-helix (residue 91–102), which is important for the lipase activity of the *LPL* protein.

Functional Analysis of Mutant LPL in 293T Cells

Western blot analysis revealed that the relative expression of mutant *LPL* was similar to that of wild-type *LPL* in 293T transfected cells, with no significant difference (Figure 5a). The quantitative PCR results indicated that the relative expression of mutant *LPL* (c.292G > A, p.A98T) is 1.58 times higher than that of

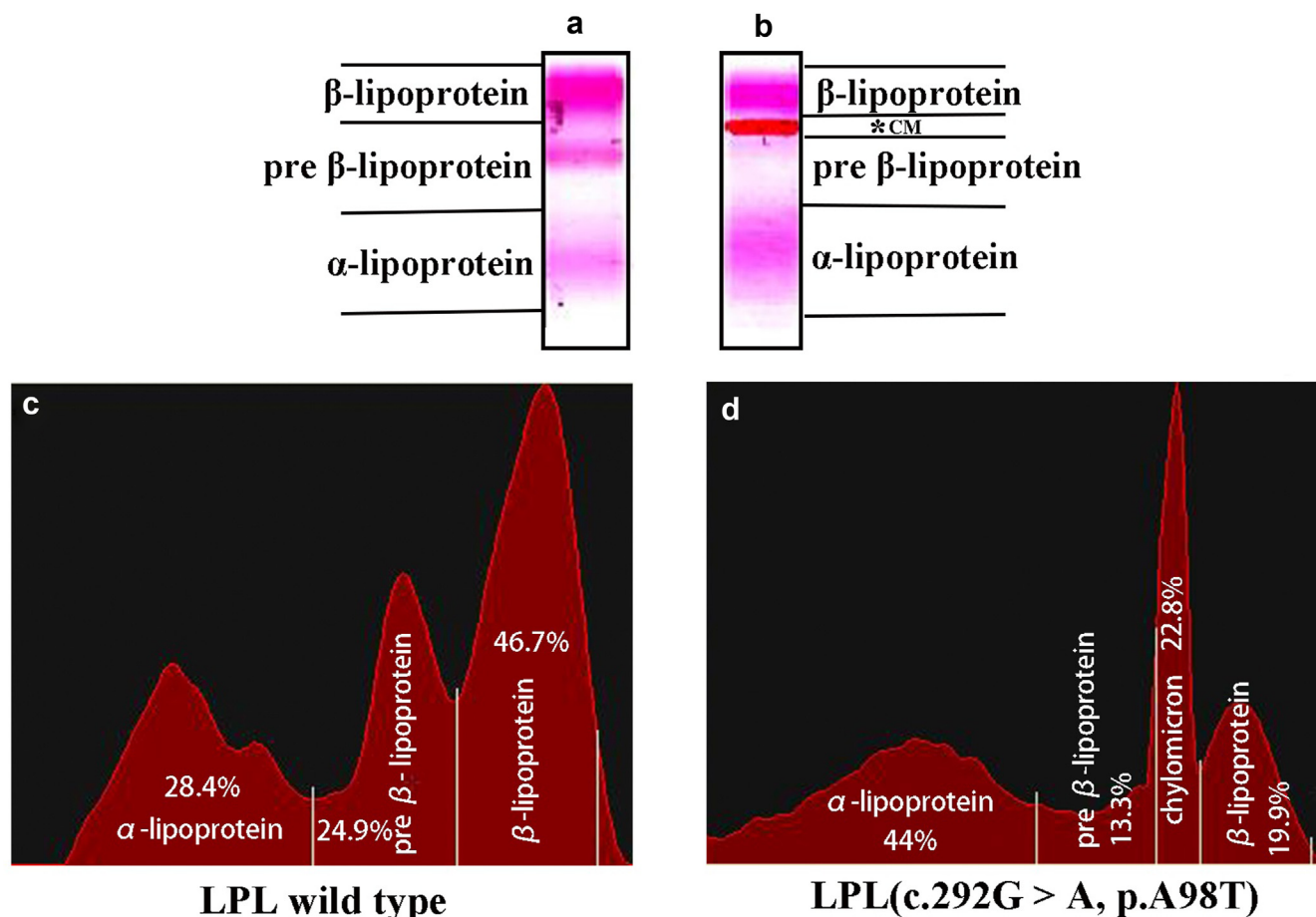


Figure 1. Serum lipoprotein profile difference between healthy control and patient with homozygous *LPL* (c.292G > A, p.A98T) variant. The lipoprotein electrophoresis results of the healthy control are shown in Figure 1a and Figure 1c. From top to bottom, the 3 bands of β -lipoprotein, pre- β -lipoprotein, and α -lipoprotein have the percentages 46.7%, 24.9%, and 28.4%, respectively. The lipoprotein electrophoresis result of the patient with homozygous *LPL* (c.292G > A, p.A98T) variant is shown in Figure 1b and Figure 1d. The chylomicron band is shown at the origin and is labeled with *. From top to bottom, the 4 bands of β -lipoprotein, chylomicron, pre- β -lipoprotein, and α -lipoprotein have the percentages 19.9%, 22.8%, 13.3%, and 44%, respectively.

wild-type *LPL* in mRNA level (Figure 5b). The *LPL* activity and mass of the cell medium decreased by 39.7% and 51.2%, respectively in the *LPL* (c.292G > A, p.A98T) when compared to the wild-type *LPL* group. These findings indicate that the medium activity and mass of mutant *LPL* (c.292G > A, p.A98T) were low or undetectable after excluding the background effect of negative control group (Figure 5c–d). There were no significant differences in cell lysates activity between the wild-type *LPL* and mutant *LPL* groups (Figure 5e).

Relative Expression, Lipid Uptake, and Oil Red O Staining in Transfected RAW264.7 Cells

Western blot analysis revealed that the relative expression of mutant *LPL* was comparable to that of wild-type *LPL* in RAW264.7 transfected cells, with no significant difference (Figure 6-Ia). The quantitative PCR results indicated that the relative expression of mutant *LPL* (c.292G > A, p.A98T) is 1.64 times higher

than that of wild-type *LPL* in mRNA level (Figure 6-Ib). Compared to the negative control group, the lipid uptake rates of the mutant *LPL* (c.292G > A, p.A98T) group and wild-type *LPL* group increased 1.39 times and 1.43 times, respectively (Figure 6-IIa, IIb, and IIc). However, no significant differences in lipid uptake rate were observed between the mutant *LPL* and wild-type *LPL* groups (Figure 6-Ic). The Oil red O staining findings were consistent with the above-stated results (Figure 6-IId, 6-IIe, and 6-IIf).

Pathogenicity Classification of the Variant

According to the ACMG guidelines, *LPL* (c.292G > A, p.A98T) variant could be classified as a likely pathogenic variant for the following evidence: (i) PS3 evidence: low lipoprotein lipase activity was observed in this mutant *LPL* group by *in vitro* functional study; (ii) PM2 evidence: homozygous *LPL* (c.292G > A, p.A98T) variant was rarely found in the Exome Variant Server, 1000 Genomes Project, and Exome Aggregation

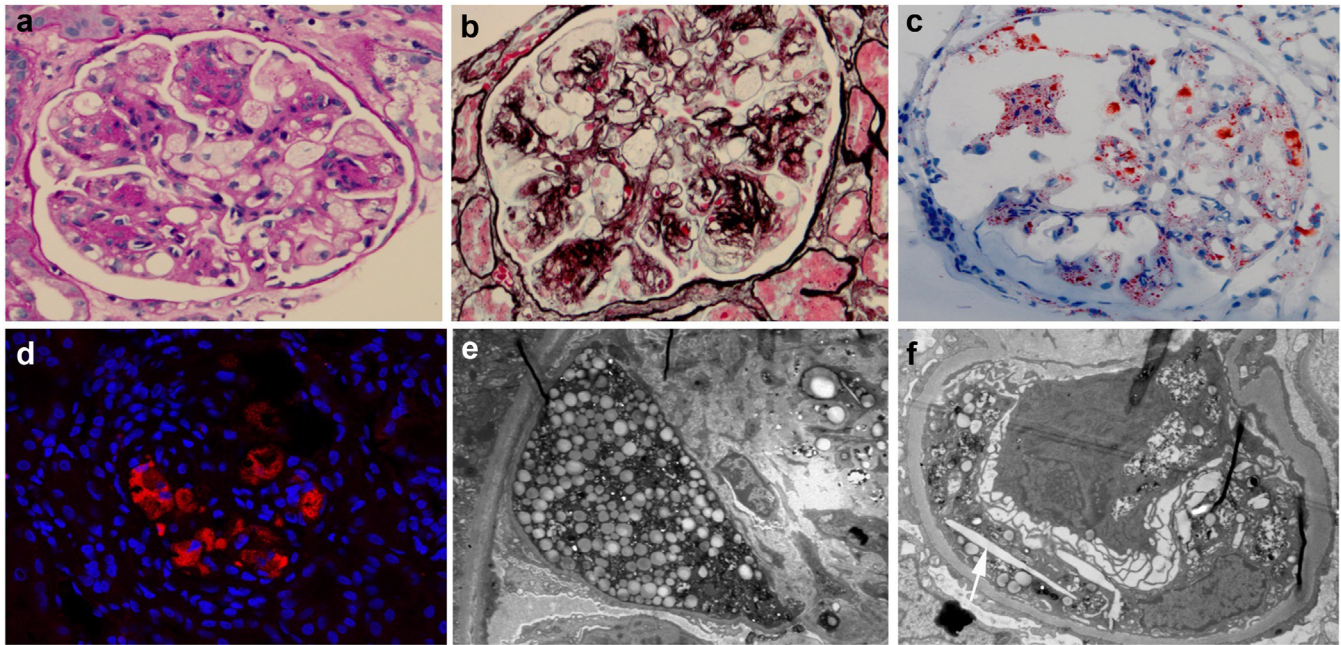


Figure 2. Pathological findings of renal biopsy specimen from patient with type I hyperlipoproteinemia. A moderate-to-severe increase in mesangial cell number and matrix, and marked foam cell infiltration in a glomerulus stained with periodic acid–Schiff stain and periodic acid–silver methenamine stain ($\times 200$) are shown in [Figure 2a](#) and [Figure 2b](#). A partial region of glomerulus positive for Oil red O staining ($\times 200$) is shown in [Figure 2c](#). A CD68-positive foam cell in a glomerulus is shown in [Figure 2d](#). Numerous lipid droplets and cholesterol clefts in the cytoplasm of foam cells (marked by white arrow) are shown in [Figure 2e](#) and [Figure 2f](#).

Consortium databases; and (iii) PP3 evidence: 3-dimensional structure and multiple bioinformatics indicated α -helix instability and deleterious effect of mutant protein.

Clinical Course

Based on the above findings, the patient was diagnosed with *LPL* homozygote-related renal lipidosis. Over the course of 1 year, his renal function and urinary protein deteriorated further, and he had recurrent pancreatitis and peritonitis. Hemodialysis was eventually initiated.

DISCUSSION

In this study, we reported a case of nephrotic syndrome with type I hyperlipoproteinemia; renal biopsy revealed severe renal lipidosis; and whole-exome sequencing identified a rare homozygous *LPL* (c.292G>A,p.A98T) mutation, which was classified as a pathogenic variant due to low secretory capacity and lipase activity. It is indicated that this homozygous *LPL* mutation was associated with the renal lesion of the patient. This is the first report of renal pathological manifestation related to homozygous *LPL* mutation.

It is known that most *LPL* variants could induce lipoprotein lipase function deficiency through decreasing its synthesis, secretory mass, and activity. The p.Ala98Thr variant is located in exon 3 and had been reported in previous studies as a simple or compound heterozygous mutation associated with

hypertriglyceridemia.^{8,18,23} Chan *et al.*¹⁸ indicated that p.Ala98Thr variant mainly affects lipoprotein lipase secretory mass and activity, which was also identified in our *in vitro* study. Our research additionally showed that the substitution of threonine for alanine may increase the H-bond conformation between LYS94 and THR98 or between LEU95 and THR98. It is reported that amino acid residue 98 is close to the first loop (residues 91–95) of LPL, which forms a hydrophobic groove around the active site.^{24,25} Therefore, the additional H-bond formation could disturb the first loop stability and further reduce lipase hydrolysis function, resulting in type I hyperlipoproteinemia.

To date, renal lesions induced by homozygous *LPL* variants have not been reported and its influence factor was unknown. It is reported that both the mutation burden and variants type could affect the phenotype of hypertriglyceridemia, and the persistent hypertriglyceridemia could aggravate organ lesion.^{4,9,26} As shown in [Supplementary Table S1](#), acute pancreatitis due to hypertriglyceridemia was the main clinical manifestation of the patients with the heterozygous *LPL* (c.292G > A, p.A98T) variant; individuals with the compound heterozygous variant presented higher TG levels than simple heterozygotes, and some simple heterozygote showed normal serum TG level. In our study, the patient who carried homozygous *LPL* (c.292G > A, p.A98T) variant showed severe type I

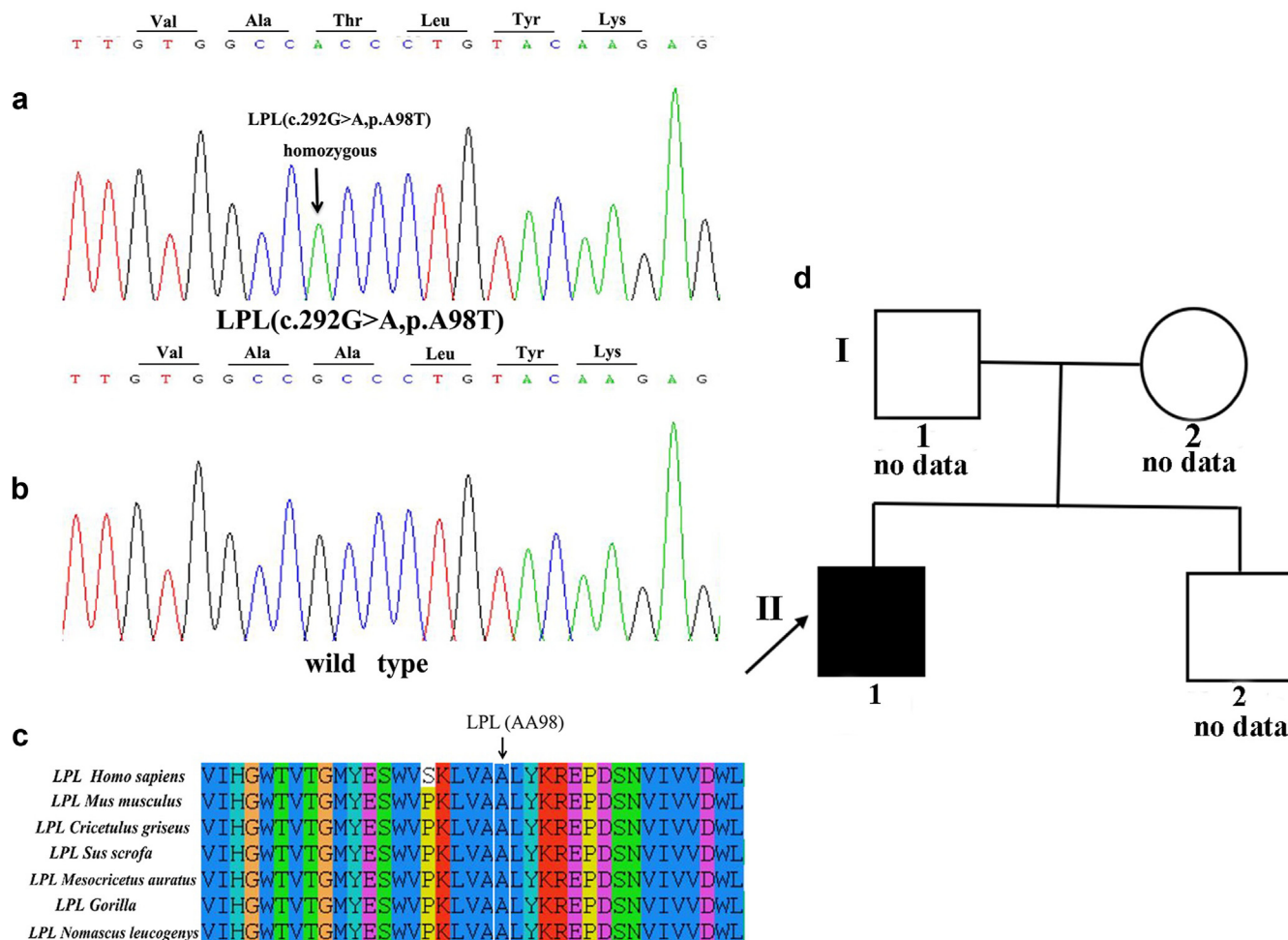


Figure 3. Homozygous *LPL* missense mutation identification, mutation site evolutionary conservation analysis, and pedigree analysis of the patient with type I hyperlipoproteinemia. Partial sequences of *LPL* exon 3 from the patient and a healthy control, respectively are shown in Figure 3A and Figure 3B. The mutation site is marked by the arrow and presented as *LPL* (c.292G > A, p.A98T). The wild-type *LPL* amino acid sequence fragments of various species are shown in Figure 3c. The white-colored box shows that the amino acid p.Ala98 is evolutionarily highly conserved. The family pedigree of the patient with type I hyperlipoproteinemia is shown in Figure 3D. An arrow represents the proband (II-1), a square represents a male individual, a circle represents a female individual, blank symbols represent unaffected family members, and black symbols represent patients homozygous for *LPL* (c. 292G > A, p.A98T). The blood samples of I-1, I-2, and II-2 are not available.

hyperlipoproteinemia, recurrent pancreatitis and peritonitis, splenomegaly and renal lesion, and the organ lesions were more severe than in simple and compound heterozygote carriers.

Moreover, diet, lifestyle and comorbidity may facilitate the development of hyperlipidemia associated renal lesion.^{27,28} The renal histopathology of patients with diabetic nephropathy who have hyperlipidemia revealed massive foam cell infiltration in addition to the typical manifestation of homogeneous and diffuse glomerular basement membrane thickening. It is indicated that diabetes mellitus may facilitate the progression of hyperlipidemia associated renal lesion. In this study, both the diabetes mellitus history and typical glomerular basement membrane thickening pathological manifestation were absent in this patient; therefore,

we deduce that the renal lipidosis lesion may mainly associated with the homozygous *LPL* variant. In addition, the patient was without family history of hyperlipidemia and presented renal lesion at middle age; it is likely that the environmental factors also play a critical role in the development of hyperlipidemia associated renal lesion.

In the general population, the proportion of apoE2 homozygote carriers is 0.5% to 1%, and <10% of these carriers have type III hyperlipoproteinemia, which is characterized by xanthomas, and elevated plasma cholesterol and TG level.²⁹⁻³¹ It is known that apoE variants play critical roles in abnormal lipid metabolism and macrophage lipid uptake, and this condition is sometimes discussed in diabetic nephropathy and apoE2 homozygote glomerulopathy that is induced by

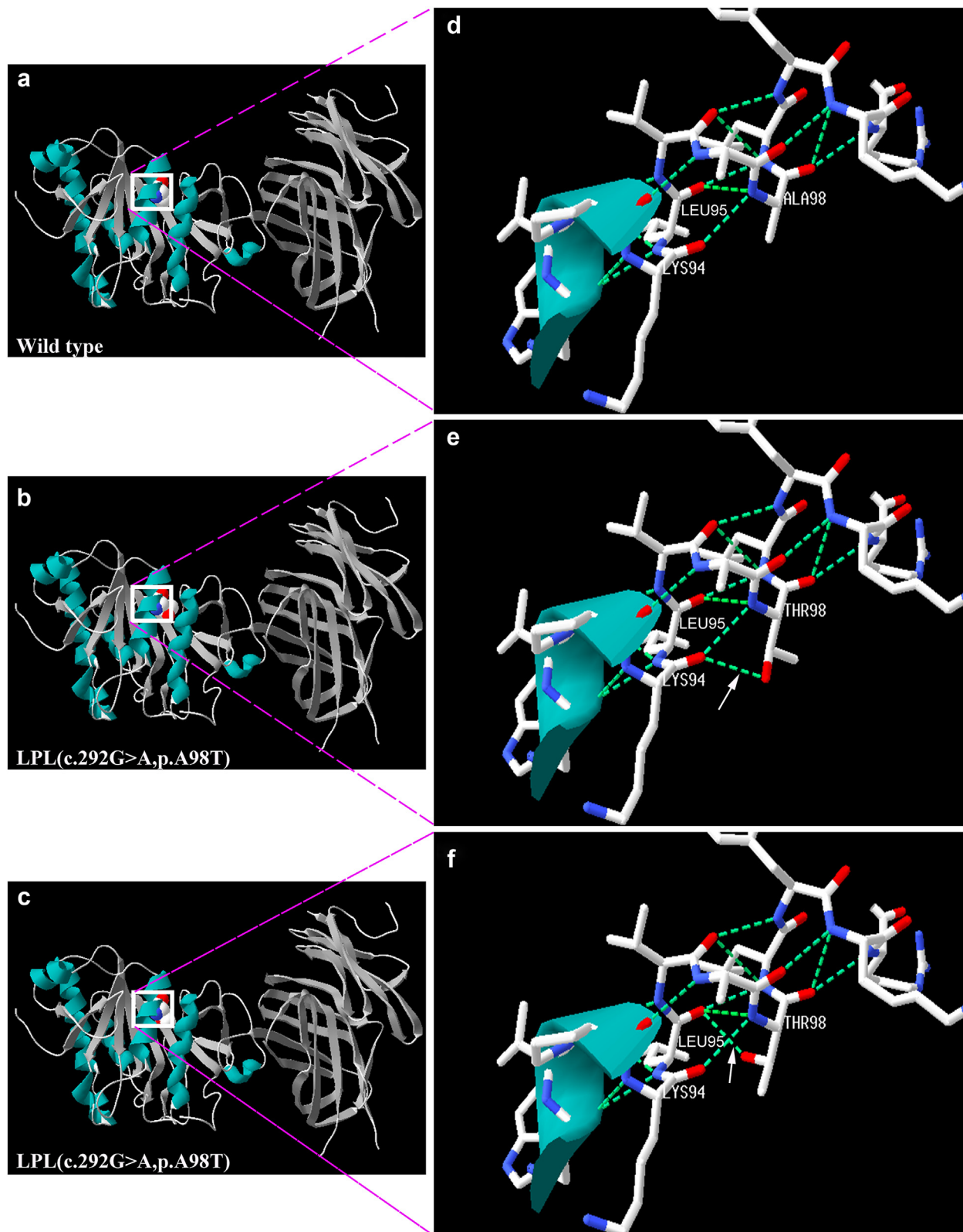


Figure 4. Protein structures of *LPL* (c.292G > A, p.A98T) and wild-type *LPL*. The 3-dimensional structure modeling of the mutant human *LPL* protein was built based on the template of the wild-type human *LPL* in complex with GPIHBP1 (Protein Data Bank entry 6E7K). The whole *LPL* protein (PDB ID: 6E7K) and the predicted *LPL* (c.292G > A, p.A98T) protein structures are shown in panels a, b, and c. Panels d, e, and f show the amplification regions of panels a, b, and c, respectively. The substitution of the amino acid Thr for Ala at site 98 may increase the side chain and H-bond number between LYS94 and THR98 or between LEU95 and THR98, causing a clash (shown by the arrow) and a conformational change.

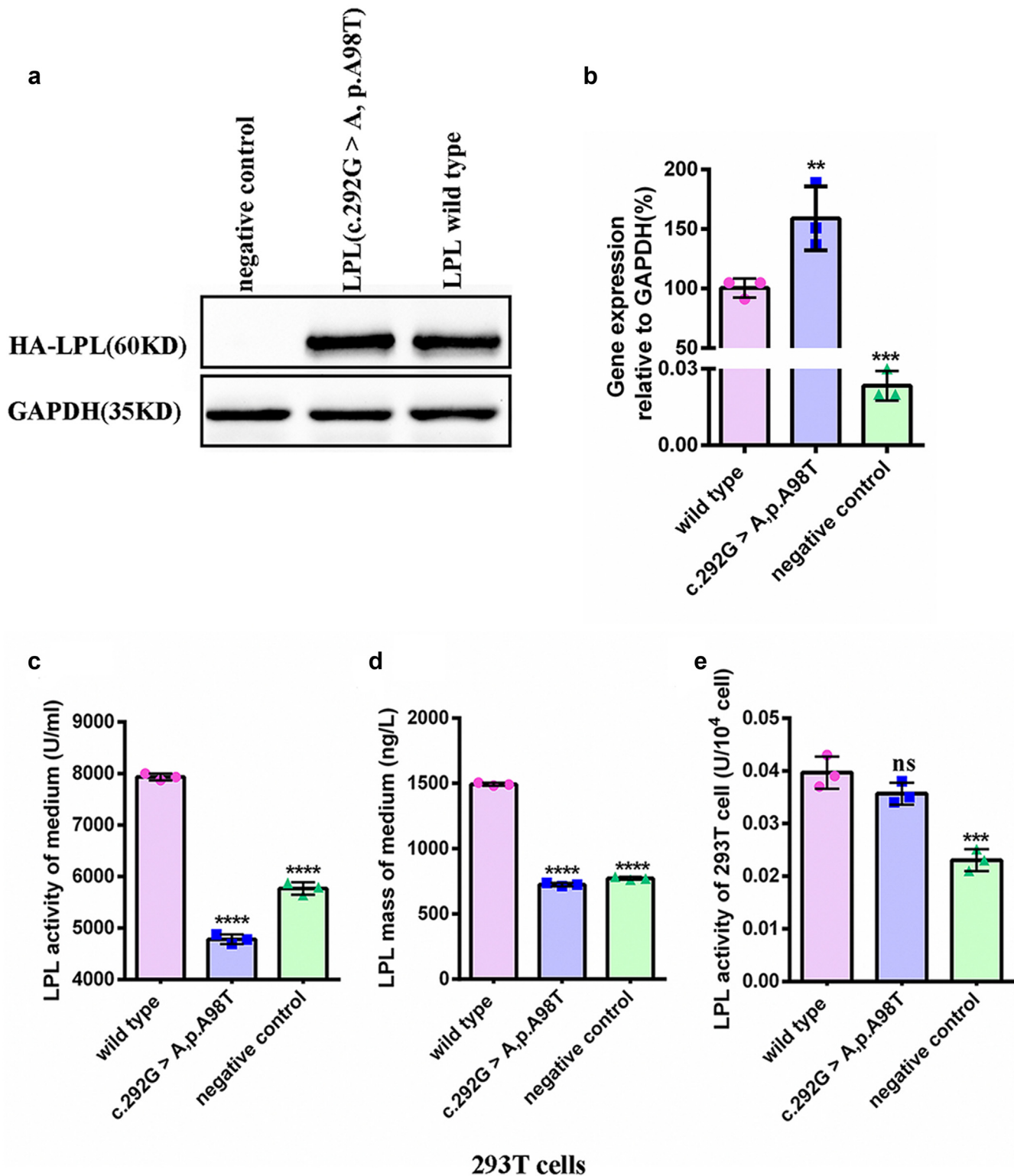


Figure 5. Functional analysis of *LPL* (c.292G > A, p.A98T) mutation in 293T cells. (a) Western blot analysis of the HA-tagged human LPL protein relative expression in various transfected 293T cells, GAPDH is used as the loading control. (b) qPCR analysis of human *LPL* relative expression in various transfected 293T cells. (c and d) the LPL activity and mass of the cell medium in 3 transfected 293T cells groups. (e) the LPL activity of the cell lysates in 3 transfected 293T cells groups. The experiments are performed with 3 replicates, data are shown as mean \pm SD, and significance tested with 1-way ANOVA for all data and indicated as * $P < 0.05$, ** $P < 0.01$, *** $P < 0.001$, **** $P < 0.0001$ to the wild-type *LPL* group.

type III hyperlipoproteinemia.^{28,32-34} It is worth pointing out that homozygous *LPL* variant in the current case also manifests renal lipodosis similar to those of

apoE2 homozygous variants. Further, it was reported that patients with type III hyperlipoproteinemia and an apoE2 homozygote background always have

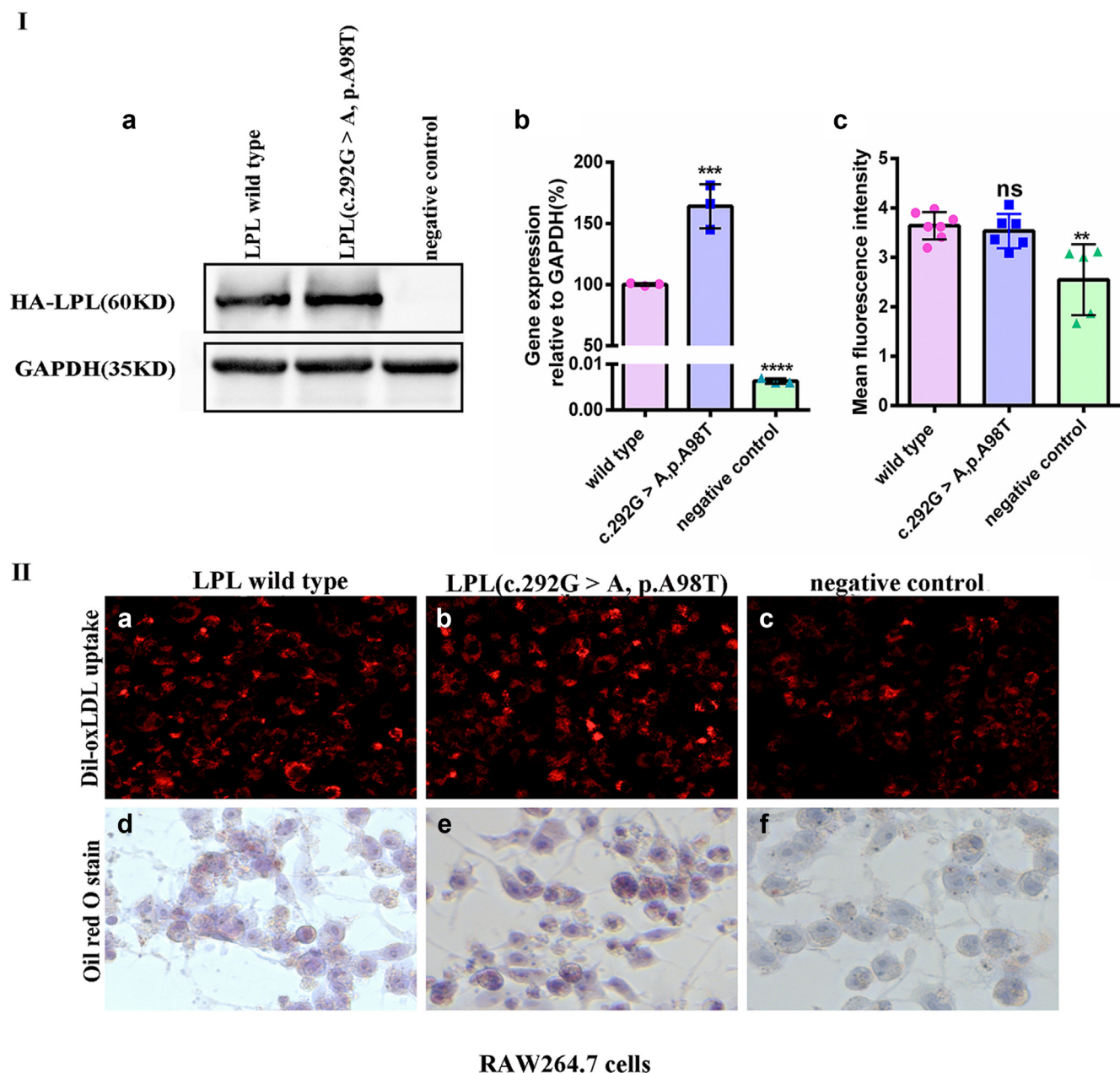


Figure 6. Analyses of *LPL* expression and lipid uptake capability of *LPL* (c.292G > A, p.A98T)-transfected RAW264.7 cells. (Ia) Western blot analysis of the HA-tagged human *LPL* protein relative expression in various transfected RAW264.7 cells, GAPDH is used as the loading control. (Ib) qPCR analysis of human *LPL* relative expression in various transfected RAW264.7 cells. (Ic) Dil-labeled mean fluorescence intensity in 3 groups. (IIa, IIb, and IIc) the Dil-labeled oxLDL uptake capability of 3 transfected RAW264.7 cells. (IIe, IIe, and IIe) the Oil-red O staining of 3 transfected RAW264.7 cells. The experiments are performed with 3 replicates, data are shown as mean \pm SD, and significance tested with 1-way ANOVA for all data and indicated as * $P < 0.05$, ** $P < 0.01$, *** $P < 0.001$, **** $P < 0.0001$ to the wild-type *LPL* group.

reduced LPL activity.^{31,35} In addition, *LPL* gene variants were identified among type II diabetes mellitus patients with renal lesion and hyperlipidemia³⁶; therefore, it is likely that macrophage infiltration in diabetic glomerulosclerosis is influenced by dyslipidemia via LPL and APOE2.

In conclusion, we presented a pathogenic *LPL* (c.292G > A, p.A98T) homozygote variant with severe renal lipodosis. This study may provide critical evidence for future research on dyslipidemia-related renal lesions.

DISCLOSURE

All the authors declared no competing interests.

ACKNOWLEDGMENTS

This work was supported by grants from the 1·3·5 project for disciplines of excellence, West China Hospital, Sichuan University (Grant number: zycj21018); the National Natural Science Foundation of China (Grant number: 81470916); the Sichuan Province Key Technology R&D Program (Grant

number: 22ZDYF1411); and Chengdu Municipal Bureau of Science and Technology (Grant number: 0040205301D74). We thank Enago Academy (www.enago.cn) for their help in language editing and Li Li, Fei Chen, and Chunjuan Bao (Institute of Clinical Pathology, West China Hospital) for processing histological staining.

SUPPLEMENTARY MATERIAL

Supplementary File (PDF)

Table S1. Clinical characteristics of reported heterozygous LPL(c.292G > A, p.A98T) variant

REFERENCES

- Basu D, Goldberg IJ. Regulation of lipoprotein lipase-mediated lipolysis of triglycerides. *Curr Opin Lipidol.* 2020;31:154–160. <https://doi.org/10.1097/MOL.0000000000000676>
- Young SG, Fong LG, Beigneux AP, et al. GPIHBP1 and lipoprotein lipase, partners in plasma triglyceride metabolism. *Cell Metab.* 2019;30:51–65. <https://doi.org/10.1016/j.cmet.2019.05.023>
- Ariza MJ, Perez-Lopez C, Almagro F, et al. Genetic variants in the LPL and GPIHBP1 genes, in patients with severe hypertriglyceridaemia, detected with high resolution melting analysis. *Clin Chim Acta.* 2020;500:163–171. <https://doi.org/10.1016/j.cca.2019.10.011>
- Rabacchi C, Pisciotta L, Cefalu AB, et al. Spectrum of mutations of the LPL gene identified in Italy in patients with severe hypertriglyceridemia. *Atherosclerosis.* 2015;241:79–86. <https://doi.org/10.1016/j.atherosclerosis.2015.04.815>
- Merkel M, Eckel RH, Goldberg IJ. Lipoprotein lipase: genetics, lipid uptake, and regulation. *J Lipid Res.* 2002;43:1997–2006. <https://doi.org/10.1194/jlr.r200015-jlr200>
- Lun Y, Sun X, Wang P, Chi J, Hou X, Wang Y. Severe hypertriglyceridemia due to two novel loss-of-function lipoprotein lipase gene mutations (C310R/E396V) in a Chinese family associated with recurrent acute pancreatitis. *Oncotarget.* 2017;8:47741–47754. <https://doi.org/10.18632/oncotarget.17762>
- Rodrigues R, Artieda M, Tejedor D, et al. Pathogenic classification of LPL gene variants reported to be associated with LPL deficiency. *J Clin Lipidol.* 2016;10:394–409. <https://doi.org/10.1016/j.jacl.2015.12.015>
- Chen T-Z, Xie S-L, Jin R, Huang ZM. A novel lipoprotein lipase gene missense mutation in Chinese patients with severe hypertriglyceridemia and pancreatitis. *Lipids Health Dis.* 2014;13:52. <https://doi.org/10.1186/1476-511X-13-52>
- Surendran RP, Visser ME, Heemelaar S, et al. Mutations in LPL, APOC2, APOA5, GPIHBP1 and LMF1 in patients with severe hypertriglyceridaemia. *J Intern Med.* 2012;272:185–196. <https://doi.org/10.1111/j.1365-2796.2012.02516.x>
- Rahalkar AR, Giffen F, Har B, et al. Novel LPL mutations associated with lipoprotein lipase deficiency: two case reports and a literature review. *Can J Physiol Pharmacol.* 2009;87:151–160. <https://doi.org/10.1139/y09-005>
- Pingitore P, Lepore SM, Pirazzi C, et al. Identification and characterization of two novel mutations in the LPL gene causing type I hyperlipoproteinemia. *J Clin Lipidol.* 2016;10:816–823. <https://doi.org/10.1016/j.jacl.2016.02.015>
- Caddeo A, Mancina RM, Pirazzi C, et al. Molecular analysis of three known and one novel LPL variants in patients with type I hyperlipoproteinemia. *Nutr Metab Cardiovasc Dis.* 2018;28:158–164. <https://doi.org/10.1016/j.numecd.2017.11.003>
- Plengpanich W, Kiattaprunvej A, Charoen S, Khovidhunkit W. Clinical and functional studies of two novel variants in the LPL gene in subjects with severe hypertriglyceridemia. *Clin Chim Acta.* 2018;487:22–27. <https://doi.org/10.1016/j.cca.2018.08.041>
- Botta M, Maurer E, Ruscica M, Romeo S, Stulnig TM, Pingitore P. Deciphering the role of V200A and N291S mutations leading to LPL deficiency. *Atherosclerosis.* 2019;282:45–51. <https://doi.org/10.1016/j.atherosclerosis.2019.01.004>
- Han P, Wei G, Cai K, et al. Identification and functional characterization of mutations in LPL gene causing severe hypertriglyceridaemia and acute pancreatitis. *J Cell Mol Med.* 2020;24:1286–1299. <https://doi.org/10.1111/jcmm.14768>
- Shi XL, Yang Q, Pu N, et al. Identification and functional characterization of a novel heterozygous missense variant in the LPL associated with recurrent hypertriglyceridemia-induced acute pancreatitis in pregnancy. *Mol Genet Genom Med.* 2020;8:e1048. <https://doi.org/10.1002/mgg3.1048>
- Taghizadeh E, Ghayour-Mobarhan M, Ferns GA, Pasdar A. A novel variant in LPL gene is associated with familial combined hyperlipidemia. *BioFactors.* 2020;46:94–99. <https://doi.org/10.1002/biof.1570>
- Chan LY, Lam CW, Mak YT, et al. Genotype-phenotype studies of six novel LPL mutations in Chinese patients with hypertriglyceridemia. *Hum Mutat.* 2002;20:232–233. <https://doi.org/10.1002/humu.9054>
- He PP, Jiang T, OuYang XP, et al. Lipoprotein lipase: biosynthesis, regulatory factors, and its role in atherosclerosis and other diseases. *Clin Chim Acta.* 2018;480:126–137. <https://doi.org/10.1016/j.cca.2018.02.006>
- Wu SA, Kersten S, Qi L. Lipoprotein lipase and its regulators: an unfolding story. *Trends Endocrinol Metab.* 2021;32:48–61. <https://doi.org/10.1016/j.tem.2020.11.005>
- Rogers MA, Atkins SK, Zheng KH, et al. Lipoprotein(a) induces vesicular cardiovascular calcification revealed with single-extracellular vesicle analysis. *Front Cardiovasc Med.* 2022;9:778919. <https://doi.org/10.3389/fcvm.2022.778919>
- Wu H, Yang J, Liu YQ, et al. Lipoprotein glomerulopathy induced by ApoE Kyoto mutation in ApoE-deficient mice. *J Transl Med.* 2021;19:97. <https://doi.org/10.1186/s12967-021-02765-x>
- Xie SL, Chen TZ, Huang XL, et al. Genetic variants associated with gestational hypertriglyceridemia and pancreatitis. *PLoS One.* 2015;10:e0129488.
- Dugi KA, Dichek HL, HnL, Santamarina-Fojo S. Human hepatic and lipoprotein lipase: the loop covering the catalytic site mediates lipase substrate specificity. *J Biol Chem.* 1995;270:25396–25401. <https://doi.org/10.1074/jbc.270.43.25396>
- van Tilbeurgh H, Roussel A, Lalouel JM, Cambillau C. Lipoprotein lipase. Molecular model based on the pancreatic lipase x-ray structure: consequences for heparin binding and catalysis. *J Biol Chem.* 1994;269:4626–4633. [https://doi.org/10.1016/S0021-9258\(17\)41822-9](https://doi.org/10.1016/S0021-9258(17)41822-9)

26. Chokshi N, Blumenschein SD, Ahmad Z, Garg A. Genotype-phenotype relationships in patients with type I hyperlipoproteinemia. *J Clin Lipidol*. 2014;8:287–295. <https://doi.org/10.1016/j.jacl.2014.02.006>
27. Agrawal S, Zaritsky JJ, Fornoni A, Smoyer WE. Dyslipidaemia in nephrotic syndrome: mechanisms and treatment. *Nat Rev Nephrol*. 2018;14:57–70. <https://doi.org/10.1038/nrneph.2017.155>
28. Saito T, Matsunaga A, Fukunaga M, Nagahama K, Hara S, Muso E. Apolipoprotein E-related glomerular disorders. *Kidney Int*. 2020;97:279–288. <https://doi.org/10.1016/j.kint.2019.10.031>
29. Smelt AHM, Beer Fd. Apolipoprotein E and familial dysbeta-lipoproteinemia: clinical, biochemical, and genetic aspects. *Semin Vasc Med*. 2004;4:249–257. <https://doi.org/10.1055/s-2004-861492>
30. Chuang TY, Chao CL, Lin BJ, Lu SC. Gestational hyperlipidemic pancreatitis caused by type III hyperlipoproteinemia with apolipoprotein E2/E2 homozygote. *Pancreas*. 2009;38:716–717. <https://doi.org/10.1097/MPA.0b013e3181ac6dc1>
31. Henneman P, van der Sman-de Beer F, Moghaddam PH, et al. The expression of type III hyperlipoproteinemia: involvement of lipolysis genes. *Eur J Hum Genet*. 2009;17:620–628. <https://doi.org/10.1038/ejhg.2008.202>
32. Geisel J, Bunte T, Bodis M, Oette K, Herrmann W. Apolipoprotein E2/E2 genotype in combination with mutations in the LDL ReceptorGene causes type III hyperlipoproteinemia. *Clin Chem Lab Med*. 2002;40:475–479. <https://doi.org/10.1515/CCLM.2002.082>
33. Beer Fd, Stalenhoe; AFH, N. Hoogerbrugge. Expression of Type III hyperlipoproteinemia in apolipoprotein E2 (Arg1583Cys) homozygotes is associated with hyperinsulinemia. *Arterioscler Thromb Vasc Biol*. 2002;22:294–299.
34. Kawanishi K, Sawada A, Ochi A, et al. Glomerulopathy with homozygous apolipoprotein e2: a report of three cases and review of the literature. *Case Rep Nephrol Urol*. 2013;3:128–135. <https://doi.org/10.1159/000356849>
35. Brümmer D, Evans D, Greten DBH, Greten H, Beisiegel U, Mann WA. Expression of type III hyperlipoproteinemia in patients homozygous for apolipoprotein E-2 is modulated by lipoprotein lipase and postprandial hyperinsulinemia. *J Mol Med (Berl)*. 1998;76:355–364. <https://doi.org/10.1007/s001090050227>
36. Mattu RK, Trevelyan J, Needham EW, et al. Lipoprotein lipase gene variants relate to presence and degree of microalbuminuria in type II diabetes. *Diabetologia*. 2002;45:905–913. <https://doi.org/10.1007/s00125-002-0824-7>